



Blue excited photoluminescence of Pr doped $\text{CaBi}_2\text{Ta}_2\text{O}_9$ based ferroelectrics

Dengfeng Peng, Haiqin Sun, Xusheng Wang*, Juncheng Zhang, Mianmian Tang, Xi Yao

Functional Materials Research Laboratory, Tongji University, 1239 Siping Road, Shanghai 200092, China

ARTICLE INFO

Article history:

Received 7 June 2011

Received in revised form 5 September 2011

Accepted 6 September 2011

Available online 12 September 2011

Keywords:

Ferroelectric

Aurivillius bismuth layered-structure

Photoluminescence

LED

Multifunctional materials

ABSTRACT

Pr^{3+} doped $\text{CaBi}_2\text{Ta}_2\text{O}_9$ based bismuth layered-structure oxides were synthesized by a simple solid state reaction method. The photoluminescence properties of the samples were investigated by excitation and emission spectra. Photoluminescence excitation spectra show that the samples have broad blue excitation band located at 430–510 nm, which covers the emission wavelength of commercial blue light-emitting diode (LED) chips. Upon the excitation of 450 nm light, a novel red emission centered at 621 nm of Pr doped $\text{CaBi}_2\text{Ta}_2\text{O}_9$ makes it useful in the white LEDs. In addition, it was also found that the photoluminescence can be improved by partial substituting Sr for Ca. These Pr^{3+} doped $\text{CaBi}_2\text{Ta}_2\text{O}_9$ based ferroelectrics could possibly be used as a multifunctional material for a wide range of applications, such as integrated electro-optical devices.

© 2011 Elsevier B.V. All rights reserved.

1. Introduction

Aurivillius bismuth layered-structure ferroelectrics (BLSFs) are generally expressed as $\text{Bi}_2\text{A}_{m-1}\text{B}_m\text{O}_{3m+3} = (\text{Bi}_2\text{O}_2)^{2+}(\text{A}_{m-1}\text{B}_m\text{O}_{3m+1})^{2-}$, where A is a large 12-coordinate cation and B is a small 6-coordinate cation with a d^0 electron configuration; A can be mono-, di-, or trivalent ions or a mixture of them, B represents tetra-, penta-, or hexavalent ions, and the subscripts m and $m-1$ are the numbers of oxygen octahedron and pseudo-perovskite units in the pseudo-perovskite layers, respectively [1]. The crystal structure of BLSFs consists of pseudo-perovskite layers, which interleave bismuth oxide $(\text{Bi}_2\text{O}_2)^{2+}$ layers along the c -axis. Since the 1960s, the series of bismuth layered-structure ferroelectrics (BLSFs) have been intensively studied for their potential applications in ferroelectric, dielectric, piezoelectric, pyroelectric, electrooptic, photocatalytic and biosensing fields [2–7]. It was reported that their physical and chemical properties can be greatly enhanced by doping with rare earth elements [2,7]. On the other hand, rare earths are doped in many host materials as luminous centers to design a large number of luminescent materials [8].

In recent years, photoluminescence properties of the rare earth doped BLSFs have attracted much attention for possible integrated photoluminescent ferroelectric device applications. To date, the photoluminescence properties of rare earth Eu, Er and Tm doped BLSFs such as $\text{Bi}_4\text{Ti}_3\text{O}_{12}$ ($m=3$) [9–15], $\text{Bi}_3\text{TiNbO}_9$ ($m=2$) [16], $\text{SrBi}_2\text{Nb}_2\text{O}_9$ ($m=2$) [17], $\text{SrBi}_2\text{Ta}_2\text{O}_9$ ($m=2$) [18], $\text{CaBi}_4\text{Ti}_4\text{O}_{15}$

($m=4$) [19] and Bi_2WO_6 ($m=1$) [20], have been investigated. As reported, rare earth R^{3+} ions occupy the A site of the BLSF hosts to substitute Bi^{3+} , Sr^{2+} or Ca^{2+} ions, strong luminescence was obtained due to $f-f$ transitions of the rare earth. These rare earth doped BLSFs show novel photoluminescent properties while retaining the ferroelectric functions. So it has been of considerable importance in designing materials for integrated optoelectronic applications [9–15,18,19]. However, the photoluminescence of the rare earth doped BLSFs is only achieved under ultraviolet or infrared light excitation; there are few reports about the blue excited luminescent properties of BLSFs. Phosphors excited by blue light have been the current focus of the luminescent materials since the development of blue emitting InGaN chips (450 nm) in 1994. The blue excited phosphors are of great significance in the fields of solid state illuminant applications, which are higher efficiency, more safety and environmental friendliness than traditional incandescent and fluorescent lamps [8,21]. For these purposes, blue-excited phosphor based on Pr^{3+} -doped oxide hosts such as BaMoO_4 [22], $\text{AgLaMo}_2\text{O}_8$ [23] and SrAl_2O_4 [24] have been reported. But these oxide hosts do not exhibit electrically functional properties, which cannot meet the integrated applications, for instance, integrated optical and electrical devices.

In this paper, $\text{CaBi}_2\text{Ta}_2\text{O}_9$ based bismuth layered-structure ferroelectrics ($m=2$) being chosen as host materials, a series of different concentrations of Pr doped $\text{CaBi}_2\text{Ta}_2\text{O}_9$ ceramic powders were synthesized by a simple solid state reaction method. Their photoluminescence properties were investigated. The strongest excitation band of the samples is located at blue regions. Upon the excitation of 450 nm blue light, the sample exhibits a strong emission peak centered at 621 nm. It was also found that the photoluminescence can be improved by partial substituting Sr for Ca.

* Corresponding author. Tel.: +86 21 65980544; fax: +86 2165985179.

E-mail addresses: xs-wang@tongji.edu.cn (X. Wang), pengdengfeng1984@163.com (D. Peng).

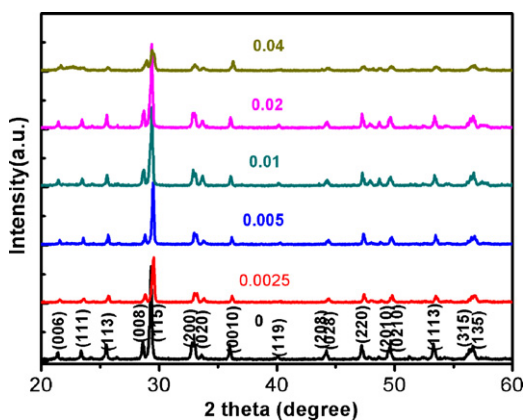


Fig. 1. XRD patterns of $\text{Ca}_{1-x}\text{Pr}_x\text{Bi}_2\text{Ta}_2\text{O}_9$ ($x=0, 0.0025, 0.005, 0.01, 0.02$ and 0.04).

To the best of our knowledge, this is the first report on a luminescence study of Pr activator in $\text{CaBi}_2\text{Ta}_2\text{O}_9$. Moreover, it is noted that $\text{CaBi}_2\text{Ta}_2\text{O}_9$ is an inherent ferroelectric [25], piezoelectric [26] and photocatalytic material [5], so $\text{CaBi}_2\text{Ta}_2\text{O}_9:\text{Pr}$ could be used as a multifunctional material for a wide range of potential applications, such as LED and integrated electro-optical devices.

2. Experimental

Powder samples with a composition of $\text{Ca}_{1-x}\text{Pr}_x\text{Bi}_2\text{Ta}_2\text{O}_9$ (where $x=0, 0.0025, 0.005, 0.01, 0.02$ and 0.04) were prepared by the conventional solid-state reaction method. Raw materials of CaCO_3 ($\geq 99.99\%$), Pr_6O_{11} ($\geq 99.99\%$), Bi_2O_3 ($\geq 99\%$) and Ta_2O_5 ($\geq 99.99\%$) were mixed thoroughly in the presence of ethanol. After drying, the mixture was pre-fired at 850°C for 2 h in air, then crushed, and sintered at 1180°C for 4 h in air. The crystal structure was identified by an X-ray diffractometer (XRD; D8 Advance, Bruker AXS GmbH) with $\text{Cu K}\alpha$ radiation ($\lambda=0.154056$ nm), tube voltage 40 mV, tube current 40 mA. The XRD profiles of $\text{Ca}_{1-x}\text{Pr}_x\text{Bi}_2\text{Ta}_2\text{O}_9$ samples were collected in the range $20^\circ < 2\theta < 60^\circ$. A step size of 0.02° (2θ) was used with scanning speed of $6^\circ/\text{min}$, the scanned refinement XRD patterns of $(\text{Ca}_{1-x}\text{Sr}_x)_{0.98}\text{Pr}_{0.02}\text{Bi}_2\text{Ta}_2\text{O}_9$ samples were recorded with scanning speed of $0.2^\circ/\text{min}$. The excitation and emission spectra of the phosphors were recorded on a PerkinElmer LS-55 luminescence spectrometer (PerkinElmer Co. Ltd., USA) equipped with a xenon lamp. The luminescent properties of all the phosphors were studied at room temperature.

3. Results and discussion

Fig. 1 shows XRD patterns of $\text{Ca}_{1-x}\text{Pr}_x\text{Bi}_2\text{Ta}_2\text{O}_9$ varying with Pr concentrations. XRD patterns of all samples match well with the standard diffraction pattern data of $\text{CaBi}_2\text{Ta}_2\text{O}_9$ and were indexed based on an orthorhombic lattice with the $A2_1am$ space group by using the JCPDS PDF database (PDF#49-0608). These XRD patterns were also found to be consistent with that reported in Refs. [5,26], indicating that those compounds consist of a pure phase of bismuth layered structure with $m=2$, and Pr was successfully doped into the $\text{CaBi}_2\text{Ta}_2\text{O}_9$ host to form solid solutions. In $\text{ABi}_2(\text{Nb,Ta})_2\text{O}_9$ BLSF compounds, it was confirmed that the $(\text{Bi}_2\text{O}_2)^{2+}$ layers were hard to substitute, while the A sites of pseudo-perovskite layers were able to accommodate a large variety of cations [27–29]. Previous study showed that for a large amount of Pr ions up to $x=0.15$ added in $\text{Sr}_{1-x}\text{Pr}_x\text{Bi}_2\text{Ta}_2\text{O}_9$ solid solution, the sample can keep pure BLSF crystal structure without second phase [27]. The crystal structure of $\text{CaBi}_2\text{Ta}_2\text{O}_9$ is similar to $\text{SrBi}_2\text{Ta}_2\text{O}_9$, so it is not strange for $\text{Ca}_{1-x}\text{Pr}_x\text{Bi}_2\text{Ta}_2\text{O}_9$ with lower Pr contents (≤ 0.04) show single phase.

Photoluminescence excitation spectra (PLES) of $\text{Ca}_{1-x}\text{Pr}_x\text{Bi}_2\text{Ta}_2\text{O}_9$ with $x=0.0025, 0.005, 0.01, 0.02$ and 0.04 are shown in Fig. 2. The excitation spectra of $\text{Ca}_{1-x}\text{Pr}_x\text{Bi}_2\text{Ta}_2\text{O}_9$ monitored at $\lambda_{\text{em}}=621$ nm, show sharp lines around 430–510 nm regions, corresponding to the f–f transitions from the $^3\text{H}_4$ ground state to the $^3\text{P}_J$ ($J=0, 1, 2$) excited states of Pr^{3+} . The intense sharp

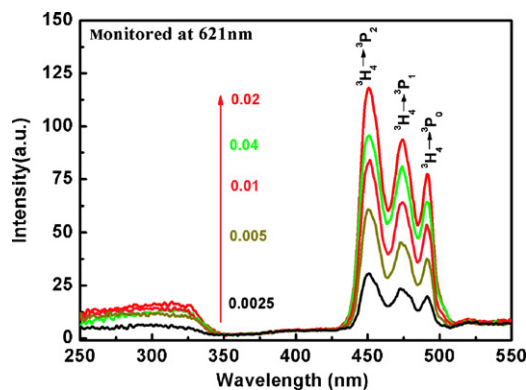


Fig. 2. Excitation spectra of $\text{Ca}_{1-x}\text{Pr}_x\text{Bi}_2\text{Ta}_2\text{O}_9$ ($x=0, 0.0025, 0.005, 0.01, 0.02$ and 0.04) monitored at 621 nm.

peaks around 450, 474 and 492 nm are due to the $^3\text{H}_4 \rightarrow ^3\text{P}_2$, $^3\text{H}_4 \rightarrow ^3\text{P}_1$ and $^3\text{H}_4 \rightarrow ^3\text{P}_0$ transitions, respectively [22–24]. It can be seen from the excitation spectra that a band located at 250–340 nm is relatively low, which is not related to any of the transition in the energy levels of Pr^{3+} ions; rather it can only be associated with the electronic transition within the host solid. The band gap (E_g) of $\text{CaBi}_2\text{Ta}_2\text{O}_9$ host is about 3.67 eV at room temperature [5], corresponding to the absorption edge at approximately 340 nm. The relative excitation intensity of the f–f transitions is higher than that of the band to band excitation of the host, indicating that the transitions in the Pr^{3+} energy levels are more dominant than the band to band excitation. This novel blue excited luminescent $\text{Ca}_{1-x}\text{Pr}_x\text{Bi}_2\text{Ta}_2\text{O}_9$ may be useful in solid state lighting which is based on the combination of blue LEDs and blue exciting phosphors.

Fig. 3 is photoluminescence emission spectra of $\text{Ca}_{1-x}\text{Pr}_x\text{Bi}_2\text{Ta}_2\text{O}_9$ with $x=0.0025, 0.005, 0.01, 0.02$ and 0.04 . By 450 nm excitation, the $\text{Ca}_{1-x}\text{Pr}_x\text{Bi}_2\text{Ta}_2\text{O}_9$ exhibit five emission peaks located at 535 nm, 548 nm, 598 nm, 620 nm and 658 nm, respectively. The energy level scheme is shown in the inset of Fig. 4. When electrons are excited to $^3\text{P}_2$ levels with 450 nm excitation, they relax nonradiatively to $^3\text{P}_1$, $^3\text{P}_0$ and $^1\text{D}_2$ states and recombined to lower levels of $^3\text{H}_4$, $^3\text{H}_5$, $^3\text{H}_6$ and $^3\text{F}_2$, the red emission band centered at 621 nm and 658 nm are attributed to the $^3\text{P}_0 \rightarrow ^3\text{H}_6$ and $^3\text{P}_0 \rightarrow ^3\text{F}_2$ transitions, respectively [22–24]. The green emission located at 535 and 548 nm are attributed to the $^3\text{P}_1 \rightarrow ^3\text{H}_5$ and $^3\text{P}_0 \rightarrow ^3\text{H}_5$ transitions, respectively [30]. The weak red emission located at ~ 598 nm is due to the $^1\text{D}_2 \rightarrow ^3\text{H}_4$ transition [24,30]. From the PL emission spectra, it can be seen that the emission intensity with Pr concentration reaches its maximum at

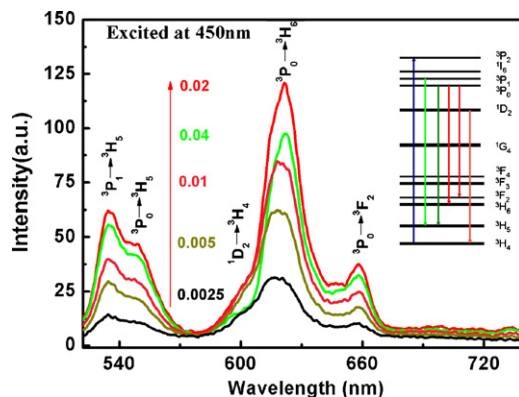


Fig. 3. Emission spectra of $\text{Ca}_{1-x}\text{Pr}_x\text{Bi}_2\text{Ta}_2\text{O}_9$ ($x=0, 0.0025, 0.005, 0.01, 0.02$ and 0.04) excited at 450 nm and the inset is its energy level scheme.

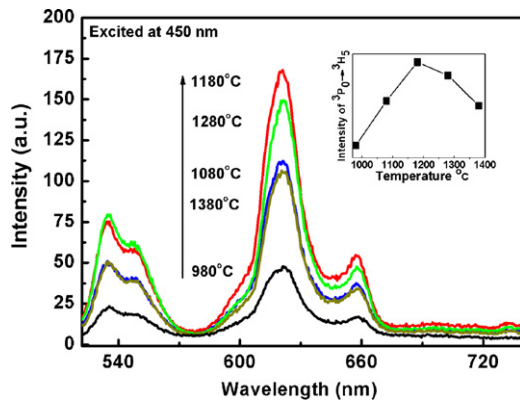


Fig. 4. Emission spectra of $\text{Ca}_{0.98}\text{Pr}_{0.02}\text{Bi}_2\text{Ta}_2\text{O}_9$ sintered at different temperatures.

$x=0.02$, and decreases contrarily with Pr increasing, owing to the concentration-quenching effect. It is known that when the doping concentration reaches a certain degree, the distance between Pr^{3+} ions became small and a fraction of energy migrated to the quenchers [22].

The effect of sintering temperature on the emission of $\text{Ca}_{0.98}\text{Pr}_{0.02}\text{Bi}_2\text{Ta}_2\text{O}_9$ was investigated. Fig. 4 shows the emission spectra of the samples prepared at different temperatures excited by 450 nm. It can be seen that the relative emission intensity of the sample is strongly affected by the sintering temperature. It is observed that with the increase of the sintering temperature, the intensity of the emission is enhanced significantly and reaches a maximum for a sample sintered at the temperature of 1180 °C and then decrease when increasing sintering temperature. It is believed that pure phase cannot be formed at the temperature lower than 1180 °C, however if the temperature is higher than 1180 °C the crystal structure is slightly destroyed due to the vaporizing of Bi^{3+} ions.

Several experiments were also carried out to investigate the influence of the substitution by Sr for Ca on the luminescent intensities of the products. In our experiments, keep other factors constantly; the samples with Ca ions partially substituting by Sr were prepared. The XRD patterns of the $(\text{Ca}_{1-x}\text{Sr}_x)_{0.98}\text{Pr}_{0.02}\text{Bi}_2\text{Ta}_2\text{O}_9$ with $x=0.1, 0.2, 0.3, 0.4$ and 0.5 revealed that the structures of $(\text{Ca}_{1-x}\text{Sr}_x)_{0.98}\text{Pr}_{0.02}\text{Bi}_2\text{Ta}_2\text{O}_9$ are pure BLSF ($m=2$) phase, suggesting that Sr^{2+} have incorporated into the $\text{Ca}_{0.98}\text{Pr}_{0.02}\text{Bi}_2\text{Ta}_2\text{O}_9$ lattice. Fig. 5 shows the scanned refinement XRD patterns near the strongest peak of (115). The (115) peak shifts to the lower-angle side with increasing Sr content. It is attributed to the lattice expansion because of the larger size of Sr^{2+} (1.44 Å, 12 CN) ion substitution for Ca^{2+} (1.34 Å, 12 CN). Meanwhile,

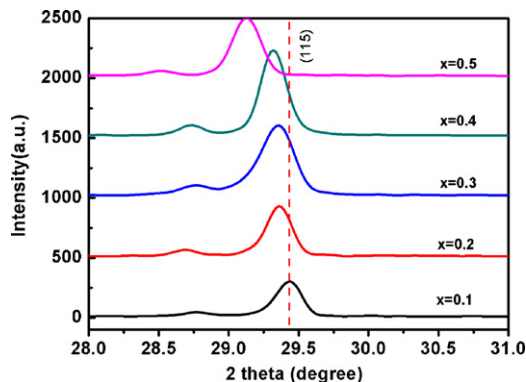


Fig. 5. XRD patterns near the strongest peak (115) of $\text{Ca}_{1-x}\text{Sr}_x\text{Pr}_{0.02}\text{Bi}_2\text{Ta}_2\text{O}_9$ ($x=0.1, 0.2, 0.3, 0.4$ and 0.5).

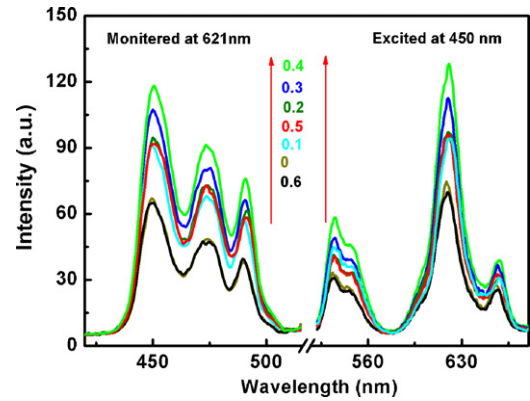


Fig. 6. Excitation and emission spectra of $\text{Ca}_{1-x}\text{Sr}_x\text{Pr}_{0.02}\text{Bi}_2\text{Ta}_2\text{O}_9$ ($x=0.1, 0.2, 0.3, 0.4, 0.5$ and 0.6).

it is observed that the increase in concentration of Sr improves the crystallinity to some extent.

The photoluminescence properties influenced by Sr substitution are also investigated. Fig. 6 shows the excitation and emission spectra of the samples. It was found that the peak positions of the excitation and emission spectra of $(\text{Ca}_{1-x}\text{Sr}_x)_{0.98}\text{Pr}_{0.02}\text{Bi}_2\text{Ta}_2\text{O}_9$ ($x=0.1, 0.2, 0.3, 0.4$ and 0.5) are not changed compared to that of the $\text{Ca}_{0.98}\text{Pr}_{0.02}\text{Bi}_2\text{Ta}_2\text{O}_9$ sample, while the increase in the emission intensity was observed with increasing of Sr, the maximum emission intensity located at 621 nm was achieved in $(\text{Ca}_{1-x}\text{Sr}_x)_{0.98}\text{Pr}_{0.02}\text{Bi}_2\text{Ta}_2\text{O}_9$ sample, higher by 174% than $\text{Ca}_{0.98}\text{Pr}_{0.02}\text{Bi}_2\text{Ta}_2\text{O}_9$. The reasons for the enhancement of the PL intensity can be ascribe to the change of the lattice symmetry. The change of the lattice symmetry will give rise to a remarkable effect on the properties of Pr^{3+} and further influence the luminescence properties [31–34], when Ca^{2+} (1.34 Å, 12 CN) ions are replaced by bigger radius Sr^{2+} ions (1.44 Å, 12 CN), the symmetry of the pseudo-perovskite units was changed [33]. As previously discussed Pr^{3+} ions dispersed in the pseudo-perovskite units of samples' crystal structure. The local environments of Pr^{3+} become more asymmetric. This change of lattice symmetry allows stronger 4f–4f emission to occur [33,34]. There are still other reasons which might influence the emission properties, such as crystallinity, particle size, defects. Among them, crystallinity might be an important factor. It is observed from the XRD patterns that the partial substitution Sr for Ca increases the crystalline of the sample to some extent. Previous reports confirmed that the luminescent intensity was improved by increasing the crystallinity in phosphors [35].

It has been noted that $\text{CaBi}_2\text{Ta}_2\text{O}_9$ BLSF ($m=2$) are also the important ferroelectric and piezoelectric materials widely used for high-temperature sensors, thin-film memory devices, and lead-free piezoelectric resonators [25,26]. It was found that the electrical properties of some $\text{ABi}_2(\text{Nb,Ta})_2\text{O}_9$ BLSF ($m=2$) could be modified by properly doping Pr^{3+} ions [29–31]. So, the ferroelectric, dielectric and piezoelectric properties of Pr doped $\text{CaBi}_2\text{Ta}_2\text{O}_9$ or $\text{Ca}_{1-x}\text{Sr}_x\text{Bi}_2\text{Ta}_2\text{O}_9$ compound will also need further study.

4. Conclusion

Pr^{3+} doped $\text{CaBi}_2\text{Ta}_2\text{O}_9$ based bismuth layered-structure ferroelectrics were synthesized by the simple solid state reaction method and their photoluminescence properties were investigated. The strongest excitation band of the samples is located at blue regions due to the f–f transitions from the $^3\text{H}_4$ ground state to the $^3\text{P}_j$ ($J=0, 1, 2$) excited states of Pr^{3+} . The samples show novel emissions excited by blue lights, upon the excitation of 450 nm light, the phosphor exhibits a strong emission peak centered at 621 nm, corresponding to the f–f transition of Pr^{3+} . It was found

that the photoluminescence can be improved by partial substituting Sr for Ca. Meanwhile, $\text{CaBi}_2\text{Ta}_2\text{O}_9$ based compounds are inherent ferroelectric, piezoelectric and photocatalytic materials, so Pr^{3+} doped $\text{CaBi}_2\text{Ta}_2\text{O}_9$ based BLSFs may be used as optical- and electro-multifunctional materials for wide range of applications.

Acknowledgements

This work was supported by the Natural Science Foundation of China (Nos. 51072136, 50932007) and Specialized Research Fund for the Doctoral Program of Higher Education (No. 20090072120034).

References

- [1] B. Aurivillius, *Ark. Kemi* 1 (1949) 499–512.
- [2] B.H. Park, B.S. Kang, S.D. Bu, T.W. Noh, J. Lee, W. Jo, *Nature (London)* 401 (1999) 682–684.
- [3] P. de Araujo, C.A. Cuchiari, J.D. McMillan, L.D.M.C. Scott, J.F. Scott, *Nature (London)* 374 (1995) 627–629.
- [4] M.D. Maeder, D. Damjanovic, N. Setier, *J. Electroceram.* 13 (2004) 385–392.
- [5] Y.X. Li, G. Chen, H.J. Zhang, Z.H. Li, J.X. Sun, *J. Solid State Chem.* 181 (2008) 2653–2659.
- [6] J.Q. Hu, Y. Yu, H. Guo, Z.W. Chen, A.Q. Li, X.M. Feng, B.M. Xi, G.Q. Hu, *J. Mater. Chem.* 21 (2011) 5352–5359.
- [7] Z.J. Zhang, W.Z. Wang, W.Z. Yin, M. Shang, L. Wang, S.M. Sun, *Appl. Catal. B: Environ.* 101 (1–2) (2010) 68–73.
- [8] Q.Y. Zhang, X.Y. Huang, *Progress Mater. Sci.* 55 (5) (2010) 353–427.
- [9] M.E. Villafuerte-Castrejón, F. Camacho-Alanís, F. González, A. Ibarra-Palos, G. González, L. Fuentes, L. Bucio, *J. Eur. Ceram. Soc.* 27 (2007) 545–549.
- [10] H. Zhou, G.H. Wu, N. Qin, D.H. Bao, *J. Am. Ceram. Soc.* 93 (8) (2010) 2109–2112.
- [11] H. Zhou, X.M. Chen, G.H. Wu, F. Gao, N. Qin, D.H. Bao, *J. Am. Chem. Soc.* 132 (2010) 1790–1791.
- [12] K.B. Ruan, X.M. Chen, L. Tong, G.H. Wu, D.H. Bao, *J. Appl. Phys.* 103 (2008) 074101.
- [13] K.B. Ruan, X.M. Chen, L. Tong, G.H. Wu, D.H. Bao, *J. Appl. Phys.* 103 (2008) 086104.
- [14] F. Gao, G.H. Wu, H. Zhou, D.H. Bao, *J. Appl. Phys.* 106 (2008) 126104.
- [15] F. Gao, G.J. Ding, H. Zhou, G.H. Wu, N. Qin, D.H. Bao, *J. Appl. Phys.* 109 (2011) 043106.
- [16] Q. Ma, Y.Y. Zhou, M.K. Lu, A.Y. Zhang, G.J. Zhou, *Mater. Chem. Phys.* 116 (2009) 315–318.
- [17] D.P. Volanti, L.V. Rosa, E.C. Paris, C.A. Paskocimas, P.S. Pizani, J.A. Varela, E. Longo, *Opt. Mater.* 31 (2009) 995–999.
- [18] K. Aizawa, Y. Ohtani, *Jpn. J. Appl. Phys.* 46 (10) (2007) 6944–6947.
- [19] W.C. Wang, H.W. Zheng, Y.F. Liu, Z.H. Li, T. Zhang, W.F. Zhang, *J. Phys. D: Appl. Phys.* 42 (2009) 105411.
- [20] M. Maczka, W. Paraguassu, A.G. Souza Filho, P.T.C. Freire, J. Mendes Filho, J. Hanuz, *Phys. Rev. B* 77 (2008) 094137.
- [21] S. Ye, F. Xiao, Y.X. Pan, Y.Y. Ma, Q.Y. Zhang, *Mater. Sci. Eng. R* 71 (2010) 1–34.
- [22] X.Y. Yang, J. Liu, H. Yang, X.B. Yu, Y.Z. Guo, Y.Q. Zhou, J.Y. Liu, *J. Mater. Chem.* 19 (2009) 3771–3774.
- [23] S. Chawla, N. Kumar, H. Chander, *J. Lumin.* 129 (129) (2009) 114–118.
- [24] Y.Q. Zhou, J. Liu, X.Y. Yang, X.B. Yu, J. Zhuang, *J. Electrochem. Soc.* 157 (3) (2010) H278–H280.
- [25] R.R. Das, P. Bhattacharya, W. Perez, R.S. Katiyar, *Appl. Phys. Lett.* 81 (21) (2002) 4052–4054.
- [26] T. Tokusu, H. Miyabayashi, Y. Hiruma, H. Nagata, T. Takenaka, *Key Eng. Mater.* 421–422 (46) (2009) 46–49.
- [27] Y. Noguchi, M. Miyayama, K. Oikawa, T. Kamiyama, M. Osada, M. Kakihana, *Jpn. J. Appl. Phys.* 41 (2002) 7062–7075.
- [28] Y. Noguchi, A. Kitamura, L.C. Woo, M. Miyayama, K. Oikawa, T. Kamiyama, *J. Appl. Phys.* 94 (10) (2003) 6749–6752.
- [29] J. Mata, A. Durán, E. Martínez, R. Escamilla, J. Heiras, J.M. Siqueiros, *J. Phys.: Condens. Matter* 18 (2006) 10509–10520.
- [30] Y. Inaguma, M. Okamoto, T. Tsuchiya, T. Katsumata, *Solid State Ionics* 179 (21–26) (2008) 788–792.
- [31] X.S. Wang, C.N. Xu, H. Yamada, *Jpn. J. Appl. Phys.* 44 (2005) L912–L914.
- [32] L. Zhang, C.N. Xu, H.S. Yamada, N. Bu, *J. Electrochem. Soc.* 157 (3) (2010) J50–J53.
- [33] J.C. Zhang, X.S. Wang, X. Yao, *J. Alloy Compd.* 498 (2010) 152–156.
- [34] W.Y. Jia, W.L. Xu, I. Rivera, A. Pérez, F. Fernández, *Solid State Commun.* 126 (3) (2003) 153–157.
- [35] A.D. Deshmukh, A. Valechha, D. Valechha, A. Kumar, D.R. Peshwe, S.J. Dhoble, *J. Lumin.* 129 (2009) 691–695.